Supporting Information

Thin laminar composite solid electrolyte with high ionic conductivity and mechanical strength towards advanced all-solid-state lithium−sulfur battery

Pengfei Zhai[a,1], Na Peng[a,1], Zeyu Sun[a], Wenjia Wu[a,*], Weijie Kou[a], Guoshi Cui[b], Kang Zhao[b], Jingtao Wang[a,c,*]

[a]School of Chemical Engineering, Zhengzhou University, Zhengzhou 450001, P. R. China

[b] Henan Kegao Radiation Chemical Technology Co., Ltd, Luoyang 471023, P. R. China

[c]Henan Institute of Advanced Technology, Zhengzhou University, 97 Wenhua Road Zhengzhou 450003, P. R. China

*To whom correspondence should be addressed: E-mail: wenjiawu@zzu.edu.cn (W.J. Wu); jingtaowang@zzu.edu.cn (J.T. Wang).

[1]These authors contributed equally to this work.

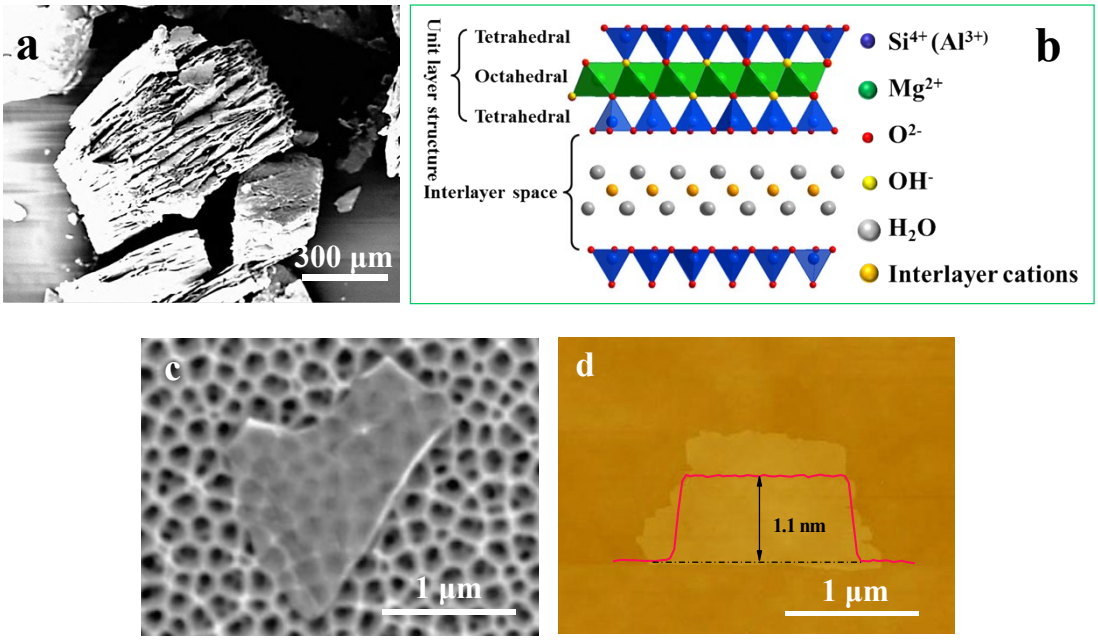

Fig. S1 (a) SEM image of vermiculite crystal. (b) Structure model of vermiculite nanosheet. (c) SEM image of vermiculite nanosheet. (d) AFM image and the corresponding height profile of vermiculite nanosheet.

Fig. S2 Photographs of the as-prepared laminar vermiculite framework.

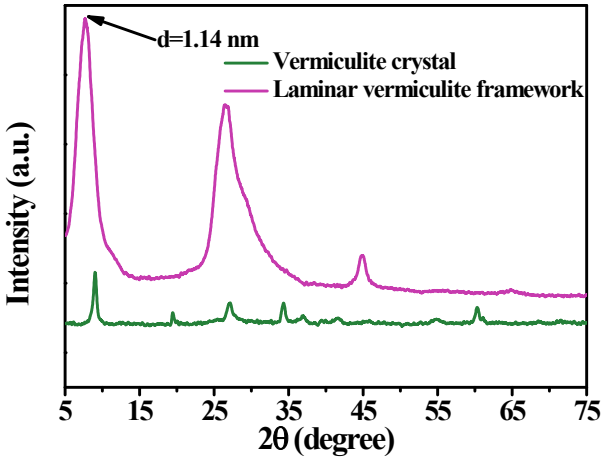

Fig. S3 XRD patterns of vermiculite crystal and laminar vermiculite framework.

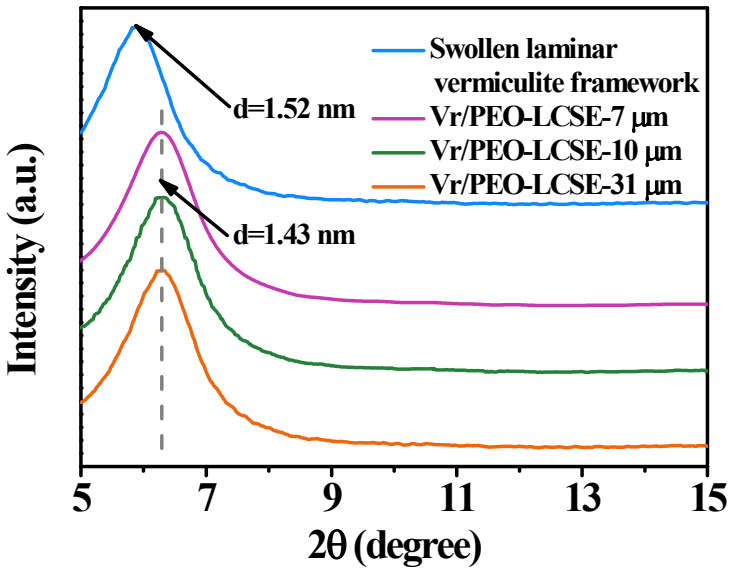

Fig. S4 XRD patterns of swollen laminar vermiculite framework and Vr/PEO-LCSE with different thicknesses.

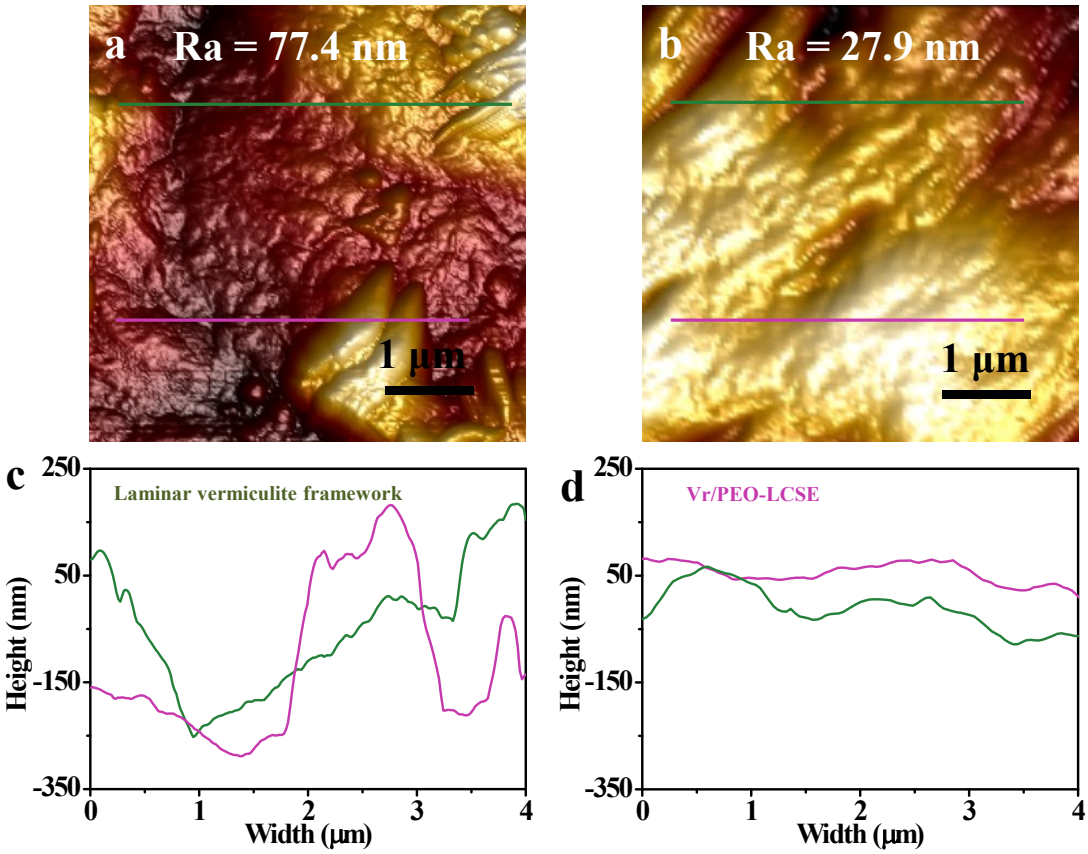

Fig. S5 (a) AFM image and (c) the corresponding height profiles of laminar vermiculite framework. (b) AFM image and (d) the corresponding height profiles of Vr/PEO-LCSE.

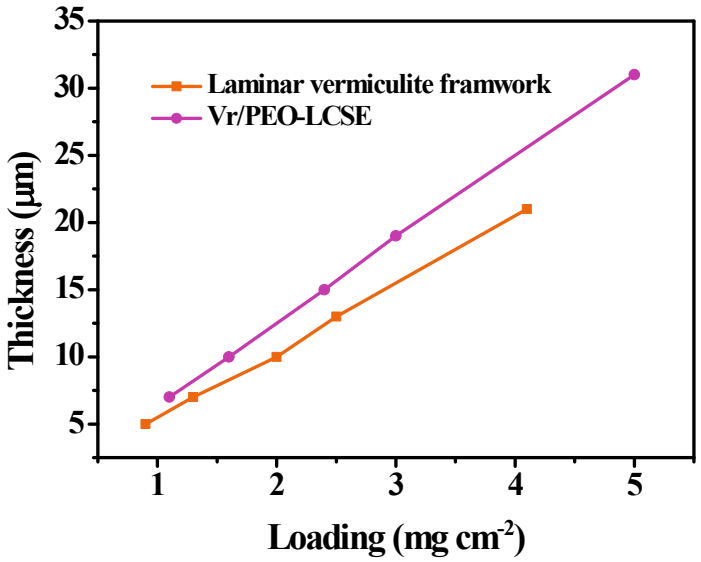

Fig. S6 The thickness of laminar vermiculite framework and Vr/PEO-LCSE as a function of vermiculite nanosheet loading amounts.

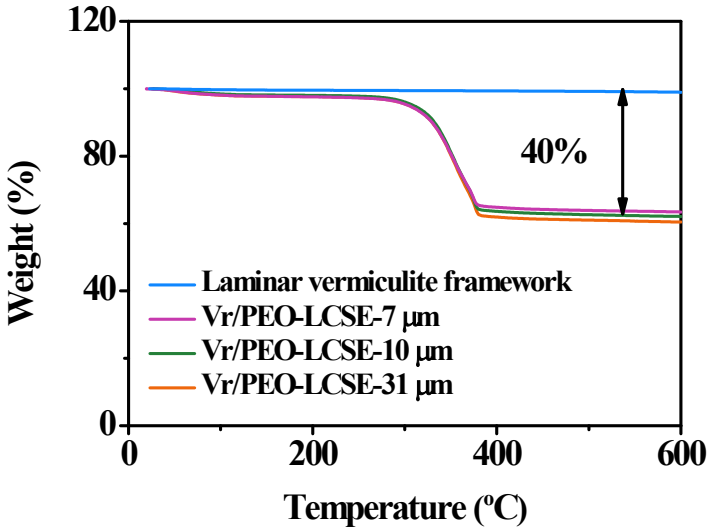

Fig. S7 TGA curves of laminar vermiculite framework and Vr/PEO-LCSE with different thicknesses.

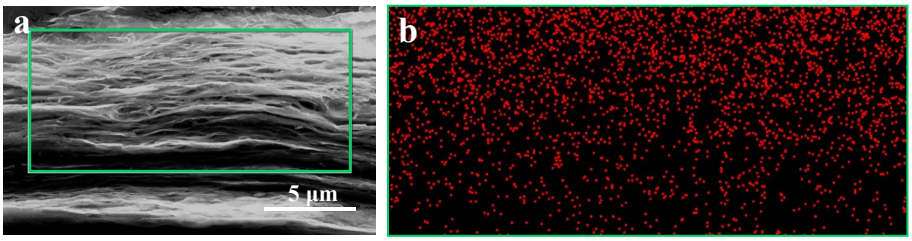

Fig. S8 (a) Cross-sectional SEM image of Vr/PEO-LCSE prepared without swelling process and (b) the corresponding EDS elemental mapping of C.

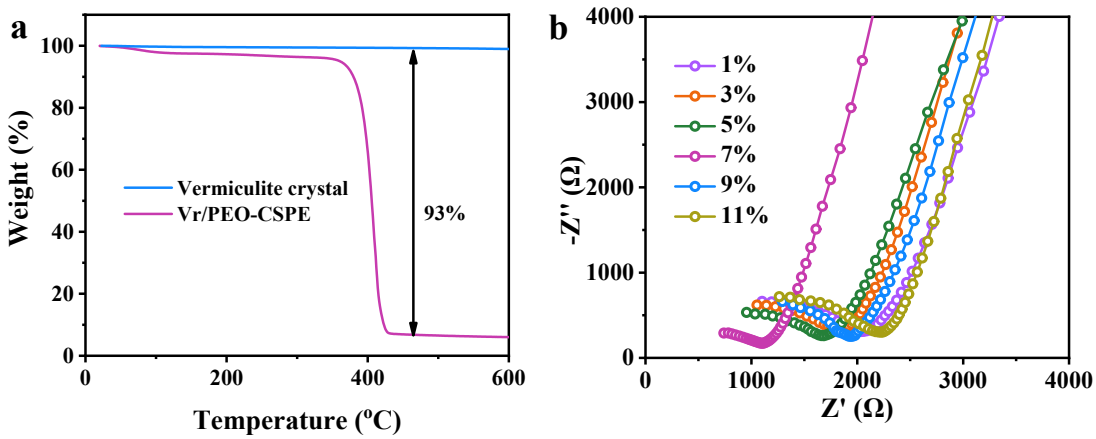

Fig. S9 (a) TGA curves of vermiculite crystal and Vr/PEO-CSPE. (b) Nyquist plots of Vr/PEO-CSPE-X (X = 1%, 3%, 5%, 7%, 9%, and 11%) at 25 °C.

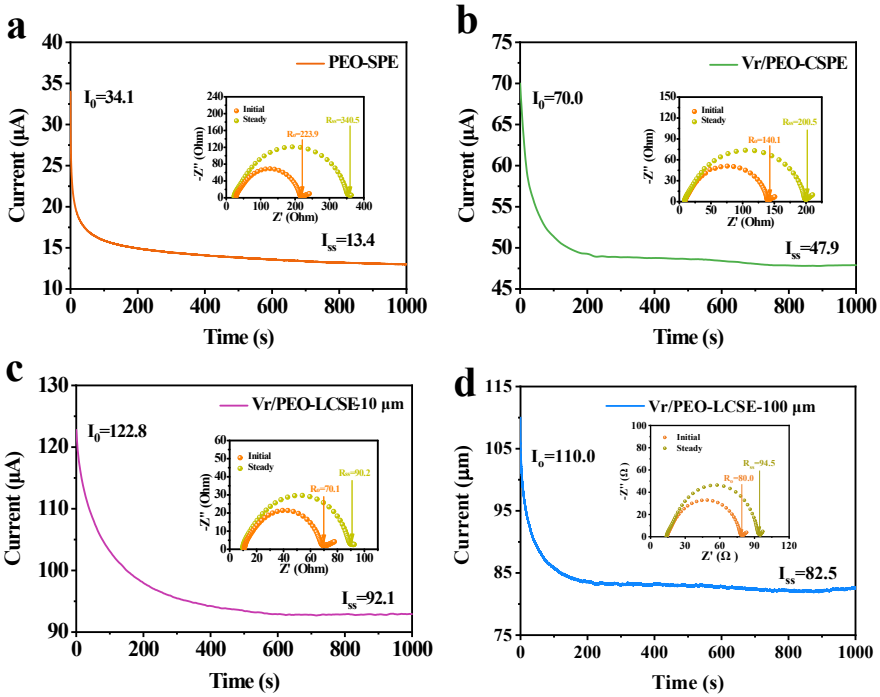

Fig. S10 The chronoamperometry curves of PEO-SPE, Vr/PEO-CSPE, Vr/PEO-LCSE-10 μm, and Vr/PEO-LCSE-100 μm at 45 °C (Inset: AC impedance curves of the corresponding cells before and after polarization).

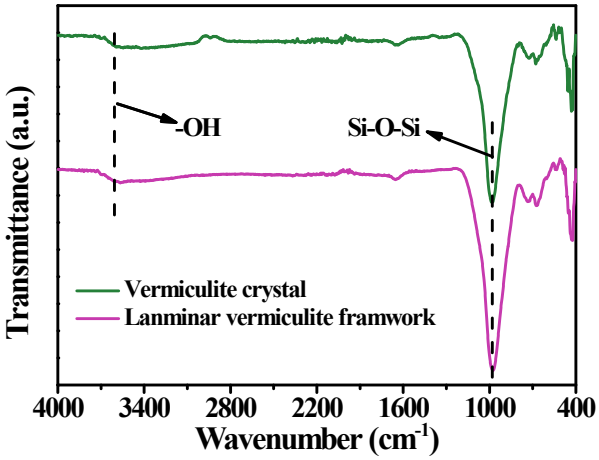

Fig. S11 FTIR spectra of vermiculite crystal and laminar vermiculite framework.

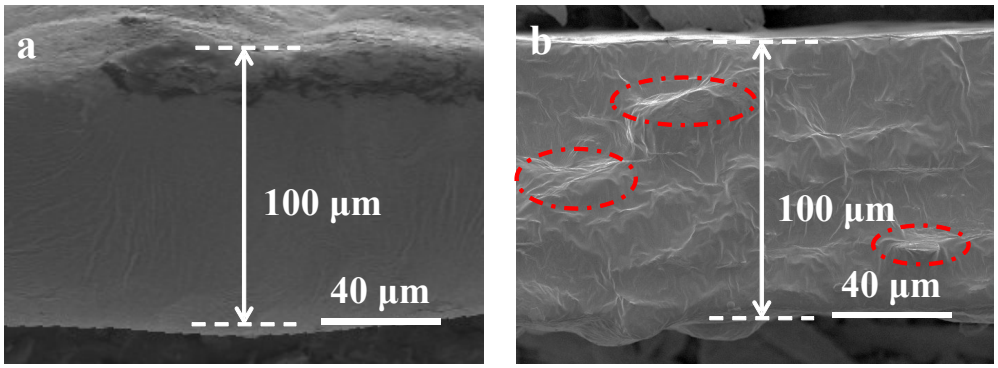

Fig. S12 Cross-sectional SEM images of (a) PEO-SPE and (b) Vr/PEO-CSPE.

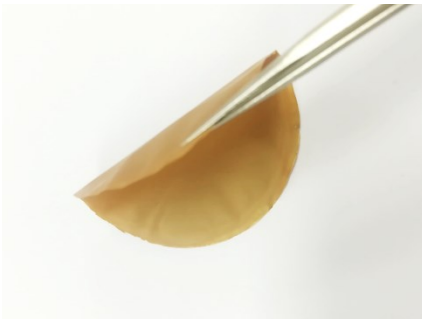

Fig. S13 Optical image of Vr/PEO-LCSE with thickness of 10 μm.

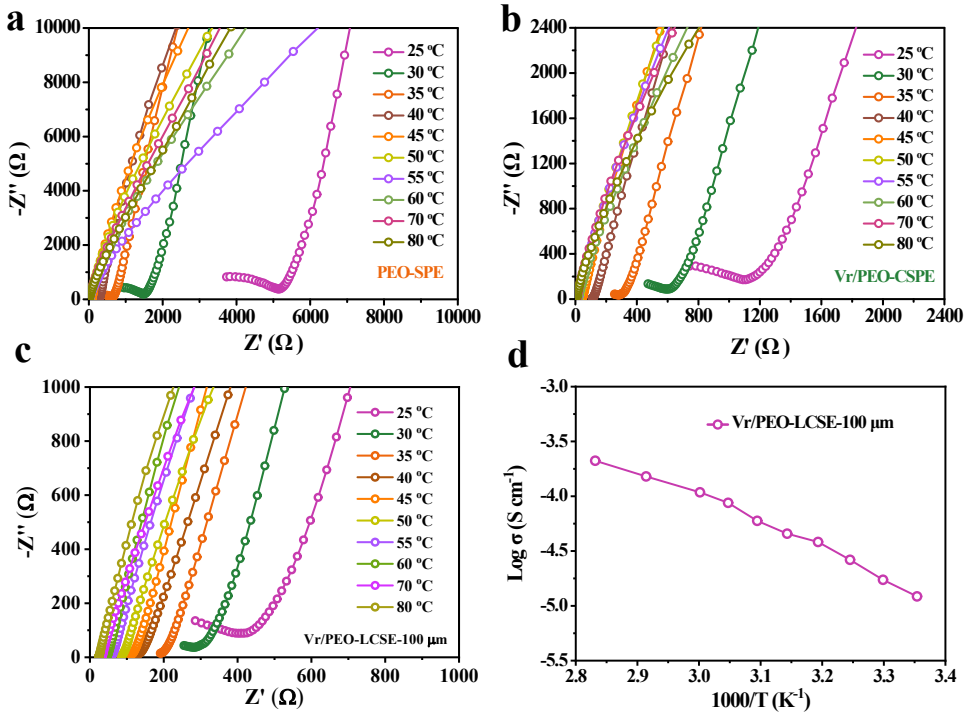

Fig. S14 Curves of (a) PEO-SPE, (b) Vr/PEO-CSPE, and (c) Vr/PEO-LCSE-100 μm at different temperatures. (d) Ionic conductivity of Vr/PEO-LCSE-100 μm.

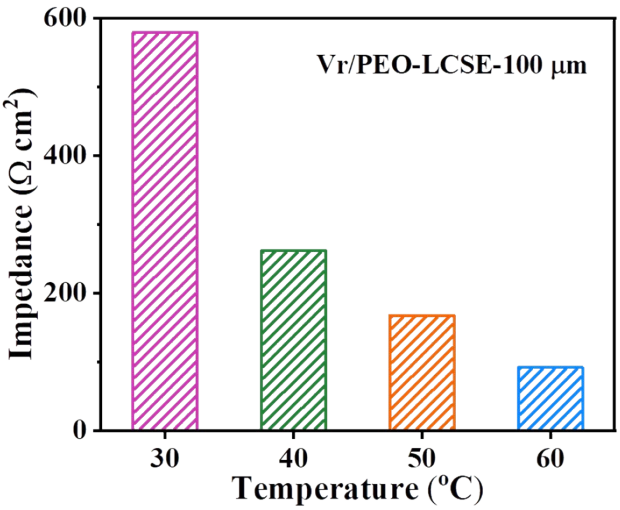

Fig. S15 ASR of Vr/PEO-LCSE-100 μm at different temperatures.

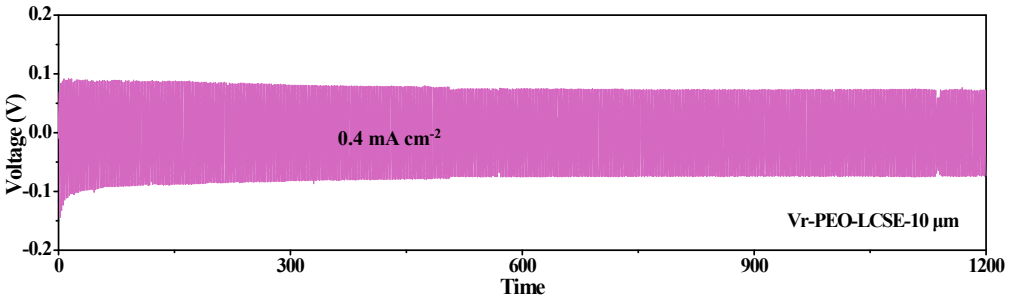

Fig. S16 Li-Li symmetric cell behavior of Vr/PEO-LCSE at 60 °C under current density of 0.4 mA cm^{-2}.

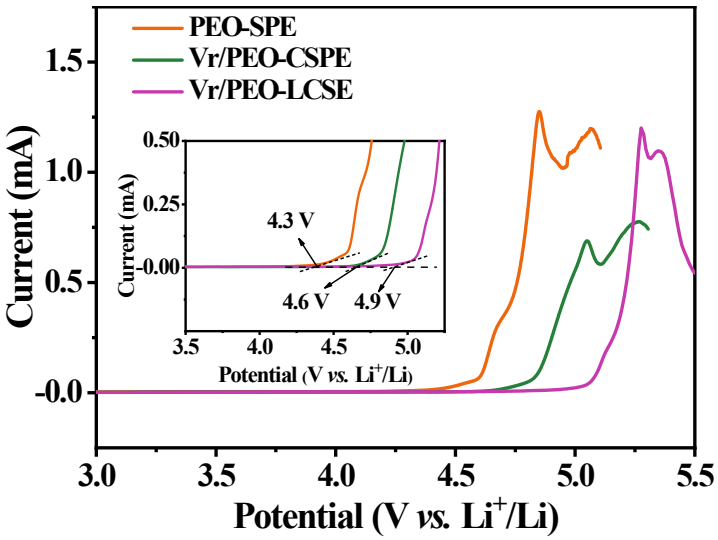

Fig. S17 Linear sweep voltammetry curves of PEO-SPE, Vr/PEO-CSPE, and Vr/PEO-LCSE.

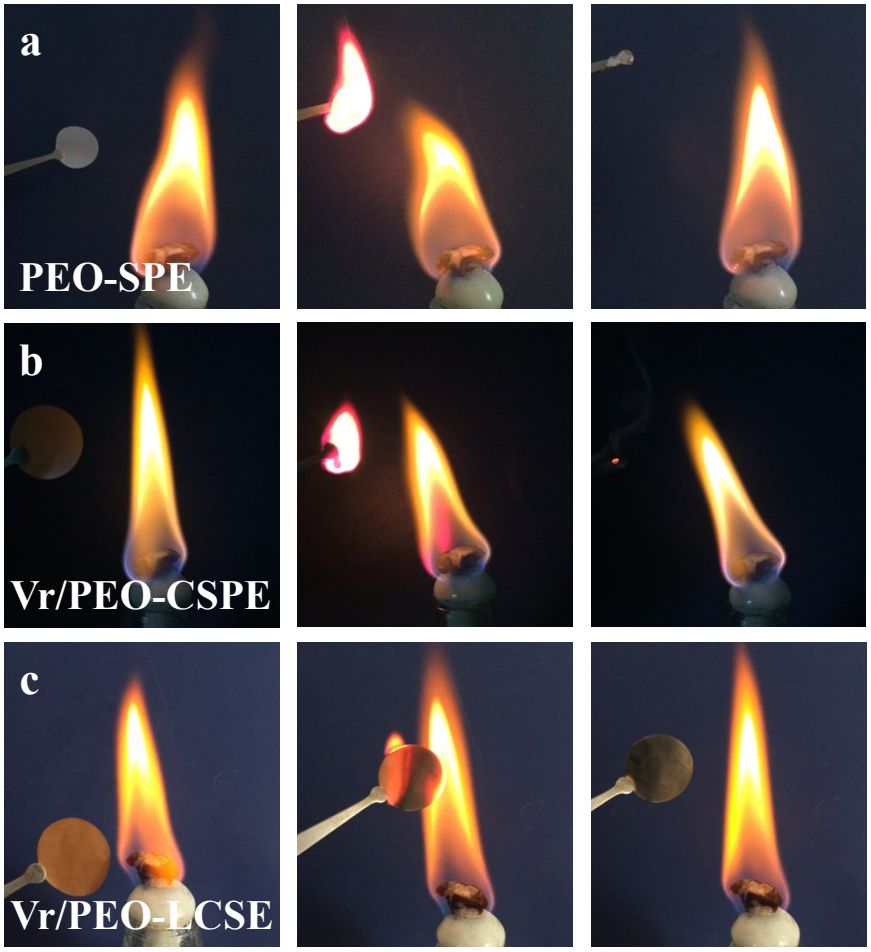

Fig. S18 Photographs of PEO-SPE, Vr/PEO-CSPE, and Vr/PEO-LCSE before and after burning.

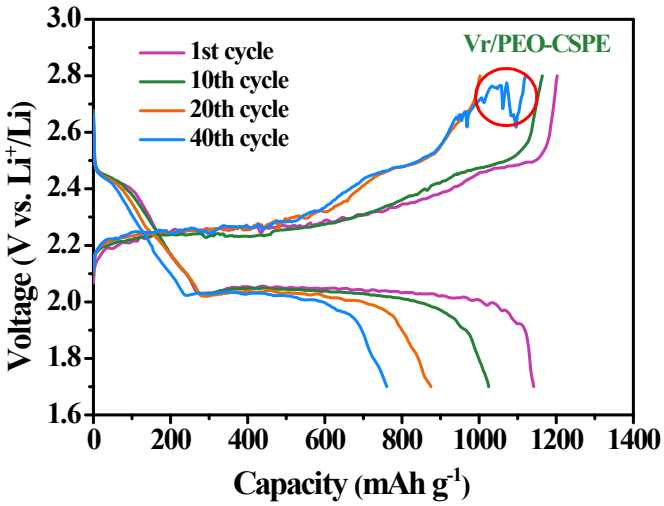

Fig. S19 Charge-discharge voltage curves of Li | Vr/PEO-CSPE | S cell at 0.05 C and 60 °C.

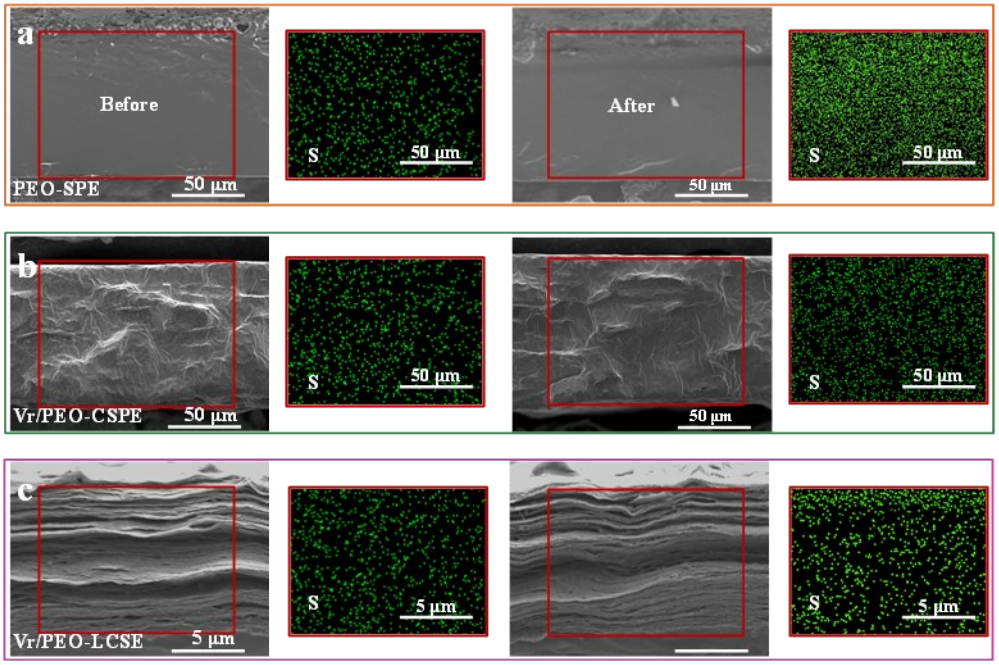

Fig. S20 Cross-sectional SEM image and the corresponding EDS elemental (S) mapping of (a) PEO-SPE, (b) Vr/PEO-CSPE, and (c)Vr/PEO-LCSE before and after 6 cycles.

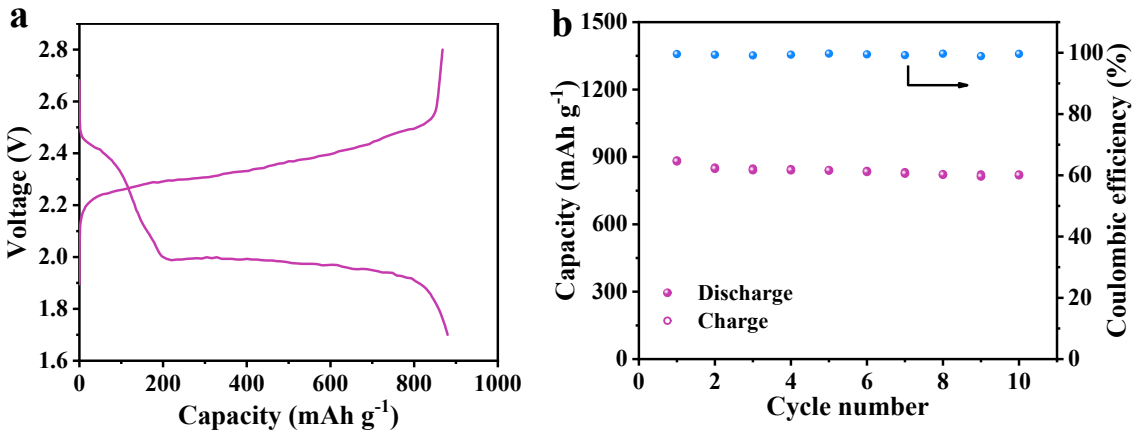

Fig. S21(a) Charge-discharge voltage curves of Li | Vr/PEO-LCSE | S cell with S loading cathode of 3.0 mg cm^{-2} at 0.1 C and 60 ^{o}C and (b) the corresponding cycling performance.

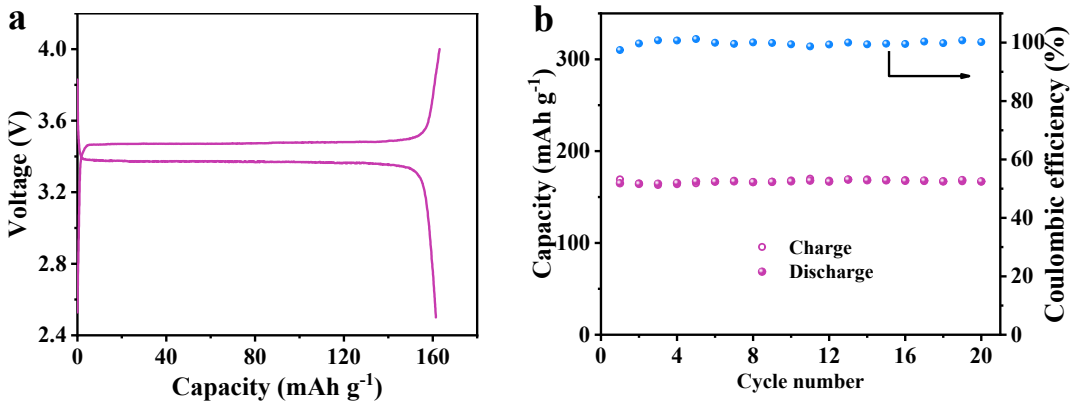

Fig. S22 (a) Charge-discharge voltage curves of Li | Vr/PEO-LCSE | LFP cell at 0.5 C and 60 °C and (b) the corresponding cycling performance.

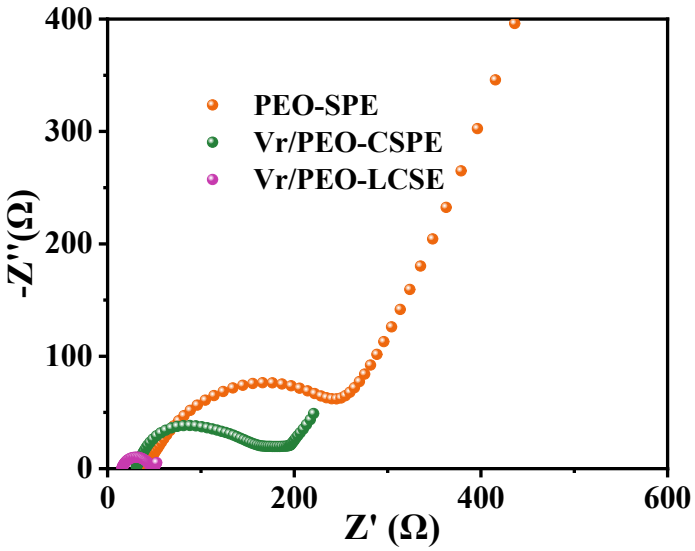

Fig. S23 The EIS impedance spectra of Li | PEO-SPE | S, Li | Vr/PEO-CSPE | S, and Li | Vr/PEO-LCSE | S cells after 5 cycles.

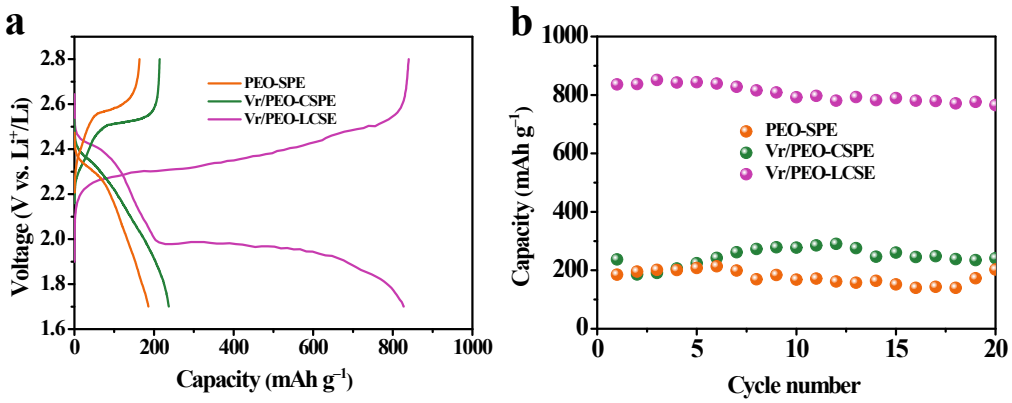

Fig. S24 (a) Charge-discharge voltage curves of Li | PEO-SPE | S, Li | Vr/PEO-CSPE | S, and Li | Vr/PEO-LCSE | S cells at 0.05 C and 45 °C and (b) the corresponding cycling performances.

Table S1 Summary of the performances of recently reported solid-state electrolytes.

Solid-state electrolyte	Conductivity (S cm^{-1})	Thickness (μm)	Tensile strength (MPa)	ARS (Ω cm^2)	Reference
PEO/LiTFSI/5% MnO_2	1.95×10^{-5} (30 °C)	90	1.27	461	1
PEO/LiTFSI/6% h-BN	7.7×10^{-6} (30 °C)	70	0.98	909	2
PEO/LiTFSI/5% g-C_3N_4	1.7×10^{-5} (30 °C)	120	1.8	706	3
PEO/LiTFSI/10% VS	2.9×10^{-5} (30 °C)	94	0.8	326	4
PEO/LiTFSI/15%SN/10% $LiAlO_2$	1.36×10^{-5} (30 °C)	80	0.88	588	5
PEO/$LiClO_4$/5% clay−CNT	3.16×10^{-5} (30 °C)	260	0.8	823	6
PEO/$LiClO_4$/1% GO	2×10^{-5} (30 °C)	240	1.27	1200	7
PEO/LiTFSI	1.3×10^{-5} (25 °C)	260	0.2	2000	8
	2.37×10^{-6} (30 °C)	80	1.25	3376	9
	5.55×10^{-6} (25 °C)	130	0.61	2342	10
	1.33×10^{-5} (30 °C)	200	0.18	1504	11
PEO/$LiClO_4$	4×10^{-6} (30 °C)	240	0.35	6000	7

Supplementary References

1. Y. Li, Z. Sun, D. Liu, Y. Gao, Y. Wang, H. Bu, M. Li, Y. Zhang, G. Gao and S. Ding, *J. Mater. Chem. A*, 2020, **8**, 2021-2032.
2. Y. Li, L. Zhang, Z. Sun, G. Gao, S. Lu, M. Zhu, Y. Zhang, Z. Jia, C. Xiao, H. Bu, K. Xi and S. Ding, *J. Mater. Chem. A*, 2020, **8**, 9579-9589.
3. Z. Sun, Y. Li, S. Zhang, L. Shi, H. Wu, H. Bu and S. Ding, *J. Mater. Chem. A*, 2019, **7**, 11069-11076.
4. W. Tang, S. Tang, C. Zhang, Q. Ma, Q. Xiang, Y.-W. Yang and J. Luo, *Adv. Energy Mater.*, 2018, **8**, 1800866.

5. N. Zhang, J. He, W. Han and Y. Wang, *J. Mater. Sci.*, 2019, **54**, 9603-9612.

6. C. Tang, K. Hackenberg, Q. Fu, P. M. Ajayan and H. Ardebili, *Nano Lett.*, 2012, **12**, 1152-1156.

7. M. Yuan, J. Erdman, C. Tang and H. Ardebili, *RSC Adv.*, 2014, **4**, 59637-59642.

8. L. Liu, J. Lyu, J. Mo, H. Yan, L. Xu, P. Peng, J. Li, B. Jiang, L. Chu and M. Li, *Nano Energy*, 2020, **69**, 104398.

9. O. Sheng, C. Jin, J. Luo, H. Yuan, H. Huang, Y. Gan, J. Zhang, Y. Xia, C. Liang, W. Zhang and X. Tao, *Nano Lett.*, 2018, **18**, 3104-3112.

10. Q. Han, S. Wang, Z. Jiang, X. Hu and H. Wang, *ACS Appl. Mater. Interfaces*, 2020, **12**, 20514-20521.

11. C. Tao, M.-H. Gao, B.-H. Yin, B. Li, Y.-P. Huang, G. Xu and J.-J. Bao, *Electrochim. Acta*, 2017, **257**, 31-39.